analytical chemistry

Article

pubs.acs.org/ac

Surface Enhanced Raman Scattering Imaging of Developed Thin-Layer Chromatography Plates

Chris E. Freye, Nichole A. Crane, Teresa B. Kirchner, and Michael J. Sepaniak*

Department of Chemistry, University of Tennessee, Knoxville, Tennessee 37996-1600, United States

ABSTRACT: A method for hyphenating surface enhanced Raman scattering (SERS) and thin-layer chromatography (TLC) is presented that employs silver−polymer nanocomposites as an interface. Through the process of conformal blotting, analytes are transferred from TLC plates to nanocomposite films before being imaged via SERS. A procedure leading to maximum blotting efficiency was established by investigating various parameters such as time, pressure, and type and amount of blotting solvent. Additionally, limits of detection were established for test analytes malachite green isothiocyanate, 4-aminothiophenol, and Rhodamine 6G (Rh6G) ranging from 10^{-7} to 10^{-6} M. Band broadening due to blotting was minimal (~10%) as examined by comparing the spatial extent of TLC-spotted Rh6G via fluorescence and then the SERS-based spot size on the nanocomposite after the blotting process. Finally, a separation of the test analytes was carried out on a TLC plate followed by blotting and the acquisition of distance × wavenumber × intensity three-dimensional TLC-SERS plots.

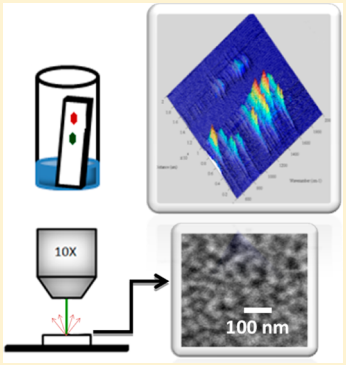

Thin-layer chromatography (TLC) is a well-established separation technique with a rich history. Poole and others have written informative reviews on the technique and its evolution.[1−5] In its simplest form, a sample is spotted via a syringe onto a planar-oriented thin layer of stationary phase (typically silica gel) and allowed to dry. The plate is then developed by allowing the mobile phase to travel along the TLC plate via capillary action. Components of the mixture will move at different rates along the TLC plate based on their differential affinity for the stationary and mobile phases leading to a spatial distribution of the individual component spots. Despite the desirability of simplicity, many modernizing advances in TLC have occurred including reduction in particle size (high performance versions, i.e., HPTLC), overpressure and electrokinetically driven development, and ultrathin stationary phase layers to mention a few.[1−5] Among the advantages of TLC is its two-dimensional (2D) nature, which allows for sample multiplexing or true 2D development with orthogonal separation modes in each dimension to increase the peak capacity (which is otherwise limited by the modest plate heights of the technique).

Detection is often based on absorbance or fluorescence: native of the separated components or enhanced via postseparation reaction with visualizing agents. In some cases, plates are covered with inorganic fluorophors to facilitate detection by spot-related fluorescence attenuation.[3−5] The developed TLC plate effectively stores the separation profile with the detection process benefiting from its static nature. Although some qualitative information resides in retardation factors (R_f) of the detected spots, component identification based on R_f is not reliable. However, TLC can be coupled with spectrometric methods such as IR, Raman, and mass spectrometry for compound specific information. Imaging detection using information rich techniques is a burgeoning area of research in planar chromatography.[6−12] In some instances, including the work described herein, separated spots are moved from the TLC plate to a detection-compatible planar medium using a blotting process. In particular, blotting has been used effectively with mass spectrometry and gas chromatography/mass spectrometry.[12−14]

Surface enhanced Raman spectroscopy (SERS) is a highly sensitive means of detection for both chemical and biological species.[15] Enhancement of the Raman signal occurs when analytes are adsorbed or in very close vicinity to nanostructured, morphologically optimized, noble metal surfaces.[16] The principle mechanism responsible for the enhancement of the Raman signal is based on an electromagnetic effect in which the field at or near the laser irradiated metal nanoparticle surface is enhanced through the development of localized surface plasmons.[17,18] Additionally, other signal enhancement can be brought about by chemical and resonance effects.[19] Under ideal conditions, these composite mechanisms can result in enhancements large enough for single molecule detection.[20−23]

Over the years, many different techniques have been developed to create a variety of SERS substrates that can be divided into two general classes, random and engineered.[24] Random substrates include metal colloidal films,[25,26] metal-island films on glass,[27−29] electrochemically roughened silver electrodes,[30,31] or polymer nanoparticles surfaces (i.e., nanocomposites).[32,33] Besides the aforementioned substrates that have random morphology, recent interest has been directed at engineered substrates with deterministic morphology. Specifically, using lithographic techniques, nanofabricated arrays have

Received: December 20, 2012
Accepted: March 24, 2013
Published: March 24, 2013

   dx.doi.org/10.1021/ac303710q | *Anal. Chem.* 2013, 85, 3991−3998

Table 1. Comparison of Solvent Evaporation Rates and Physical Properties

solvent	$T^{1}/_{2}$ (s)	dispense rate (mg/s)	η (mPa·s)	vapor pressure (torr)	ρ (g/mL)	surface tension (mN/m)	polarity index
ethanol	121	8.56	1.07	44.6	0.789	22.39	4.3
methanol	50.2	16	0.544	97.7	0.792	22.5	5.1
acetonitrile	42.5	6.27	0.343	72.8	0.787	29.1	5.8
water	–	–	1	20.1	0.998	72.86	10

been produced and implemented as SERS substrates.[34−39] Previously, our group has studied the SERS applications of random morphology polymer nanocomposites prepared by physical deposition of silver metal onto a pliable polydimethylsiloxane (PDMS) polymer.[40,41] These nanocomposites offer unique characteristics relative to other SERS substrates, including partial protection of the noble metal from oxidation (the metal is slightly submerged in the PDMS) and utilization of the PDMS material as an efficient solid-phase extractor of analyte.[41] Moreover, the composites can be molded, manipulated, and relevant herein, conformally sealed to surfaces. Despite the advantages of using nanocomposites, there are drawbacks to this substrate, most notably inhomogeneity in enhancement sites across the substrate and a limited effective surface area. In order to overcome any inhomogeneous features on the substrate, an averaging technique was used by translating the substrate back and forth a distance of 500 μm while acquiring the signal.[42]

The coupling of thin-layer chromatography and surface enhanced Raman spectroscopy (TLC-SERS) is a relatively unexplored area of separation and detection. In the late 1980s, the first report of TLC-SERS emerged.[43] After separation of the analytes on a TLC plate, silver colloid was applied through an atomized spray providing a platform for SERS imaging. This approach has also been implemented on different chemical species such as amino acids,[8] pharmaceuticals,[10] and for analysis of historical artifacts.[11] Although the atomized colloid approach provides a means of detection for TLC, there are inherent drawbacks to this system. Although the silica does not provide significant background to the SERS signal, an interaction between the TLC plate's Si−OH groups and the chemical can result in hydrogen bonding leading to a shift in the obtained spectrum.[44] Moreover, the achieved sensitivity was not great, and obviously the plate cannot be reused. Another innovative method for TLC-SERS was through the creation of silver nanorod array substrates that are then used directly for both on-chip separation and detection.[9] Silver nanorods are a proven SERS medium, but their value in chemical separations is essentially unexplored. In addition, the importance of realizing independent control of separation versus detection conditions cannot be overestimated.

In this paper, we report that the coupling of TLC-SERS can be accomplished by using conformal blotting as a novel technique to transfer analytes from a TLC plate onto a silver−polymer nanocomposite substrate. SERS imaging by rastering over the substrate provides a means to acquire information rich spectra on separated components. While SERS offers the selectivity to deal with very simple mixtures, spectral features overlap with mixtures of even modest complexity, and thus, the hyphenation of SERS with TLC, without significant detection time constraints, could prove analytically very useful. To the best of our knowledge, this is the first illustration of the use of conformal blotting of TLC components onto compliant SERS substrates. Inhomogeneity in the substrates is overcome using a translation device that also serves to reduce photodegradation of the analyte and substrate. Optimization of blotting conditions and evaluation of analytical performance of our approach are the focus of this report.

EXPERIMENTAL SECTION

Materials and Reagents. Rhodamine 6G (Rh6G) was purchased from Fisher Scientific, 4-aminothiolphenol (ATP) was purchased from Sigma−Aldrich, and malachite green isothiocyanate (MGITC) was purchased from GenoLite Biotek. All stock solutions and subsequent dilutions were prepared with ethanol (95%) from Decon Laboratories, Inc. and methanol (high-performance liquid chromatography (HPLC) grade) and acetonitrile (HPLC grade) from Fisher Scientific. Distilled water was obtained using a Barnstead 1800 (18 MΩ·cm resistivity) filter. Sigma−Aldrich was the source of TLC C-18 silica gel matrix plates.

Preparation of SERS Substrates. Sylgard 184 PDMS elastomer kits were purchased from Dow Corning and prepared as directed by manufacturer literature. The prepolymer and the curing agent were prepared in a 10:1 mass ratio, mixed thoroughly, degassed, and poured into a shallow (∼2 mm) mold. The mold was then placed in a Precision mechanical convection oven at 100 °C for 45 min. By using a physical vapor deposition system (Cooke Vacuum Products, Inc. instrument), a nominal thickness of 20 nm of silver metal (99.999% purity from Alfa Aeser) was deposited at a rate of 1.0 Å/s onto the cured PDMS films.

Blotting and Detection. Initial experiments were performed by simply submerging TLC plates in test analyte solutions for 5 min before being removed and allowed to dry at room temperature for 10 min. This allowed the analyte to uniformly coat the TLC plate and simplified evaluation of blotting parameters. After drying, the plates were sprayed with ethanol, methanol, or acetonitrile using a Preval spray gun (Home Depot). Performed manually, the solvent was sprayed left to right over the TLC plates, with one pass equaling one left to right motion of the Preval spray gun. It was determined that three passes provided the best blotting signals. The amount of solvent transferred onto the TLC plate for each trial (n = 4) yielded a relative standard deviation (RSD) about equal to 9%, demonstrating the amount of solvent sprayed on the plate was relatively consistent despite the manual operation. The rate of dispensing and subsequent evaporation of these common reversed phase organic modifiers was evaluated gravimetrically (see Table 1).

When conformal blotting, the freshly sprayed TLC plates were placed in the pressure applicator as seen in Figure 1 along with the Ag−PDMS nanocomposite. The TLC plate and nanocomposite film were separated after a specified contact time. Prior research demonstrated the effectiveness of a sample translation technique (STT) at reducing or eliminating sample and SERS substrate photodegradation.[42] That work and some studies reported herein were performed using circular (i.e., rotating)-STT by placing the substrate on a mechanical chopper (Stanford Research System, Inc., model SR540

dx.doi.org/10.1021/ac303710q | Anal. Chem. 2013, 85, 3991−3998

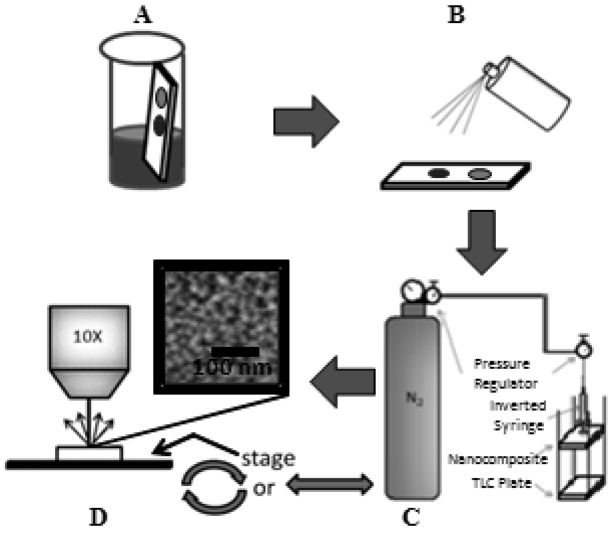

Figure 1. Schematic representation for coupling of TLC with SERS: (A) separation of analytes; (B) TLC plate sprayed with selected solvent; (C) wetted TLC plate and silver nanocomposite are conformally blotted using pressure applicator; (D) analysis by SERS (scanning electron micrograph of nanocomposite shown).

chopper controller) and operating at speeds of roughly 1000 rpm. The circular-STT is not amenable to interrogating actual TLC spots (initial or postdevelopment). In those cases, a linear translation was performed. The substrate was placed on a motorized stage (Thor Laboratories, model Z612B) and moved 500 μm back and forth at a rate of roughly 500 μm/s to create a linear-STT equivalent of circular-STT.

The nanocomposites were analyzed using a JY Horiba LabRam Raman spectrometer equipped with a Wright Instruments CCD and an ETRI helium–neon laser (633 nm). The confocal hole and slit hole of the instrument were set to 500 and 200 μm, respectively. Raman spectra were obtained using a 10× objective (0.25 NA, ∞) using 180° geometry with a 3000 cm^{-1} window centered at 1757 cm^{-1}. The scattered radiation was dispersed with 600 grooves/mm grating and processed for broad background scattering using the LabSpec 4.12 software of our Raman system. The LabRam spectrometer employs an $x-y-z$ programmable translation stage (Marzhauser Wetzlar GmbH; Wetzlar–Steindorff, Germany) for sample manipulation. Imaging was performed by a raster technique with typical stage movements in the $x-y$ dimensions of 100 μm. In an evaluation of blotting related band dispersion, analysis of undeveloped Rh6G spots on TLC plates was performed using an Ar+ laser (488 nm, 10 mW, Cyonics model 2201-20SL) for fluorescence excitation. The unfocused Ar+ laser excitation was reflected onto the TLC plate at an angle of 45°, and the LabRam spectrometer (adjusted to monitor the Rh6G emission) was used to monitor the fluorescence while the $x-y-z$ stage of the spectrometer provided a means to measure spot size on the plate.

TLC Experiments. A separation of the three test analytes was accomplished by first spotting 5×10^{-3} M ATP, 10^{-4} M Rh6G, and 10^{-6} M MGITC solutions (1 μL) onto a TLC plate using a HPLC syringe. The separation took place in a traditional development chamber using pure ethanol as the mobile phase solvent. The solvent front traveled roughly two centimeters beyond the original sample spot before the TLC plate was removed and allowed to dry before being conformally blotted using the optimized conditions. By using fluorescence and visual inspection, R_f values for band center of 0.75, 0.43, and 0.28 were determined for ATP, Rh6G, and MGTIC, respectively. Contrary to blotting and detection conditions, efforts to optimize separation conditions was minimal as it was deemed that overlapping spots permits an illustration of the selectivity advantage of SERS. By using the optimized conformal blotting procedures, the three analytes were transferred onto a silver nanocomposite and evaluated via SERS imaging with linear-STT using an acquisition time of 4 s and laser power of 1.0 mW.

RESULTS AND DISCUSSION

Instrumental Considerations. *Blotting Apparatus.* Evolution of the conformal blotting system (see Figure 1) led to a reproducible method for precisely and conveniently blotting onto nanocomposite substrates. Implementation of a stage that only moves in the z direction created a level surface upon which pressure is applied to mate the nanocomposite and TLC plate. Uneven pressure can lead to destruction of the SERS substrate as well as nonuniform blotting. Furthermore, this stage allowed for smooth separation of the nanocomposite from the TLC plate reducing physical degradation. Employing a pressurized system allowed the nanocomposite and TLC plate to be subjected to precise, controllable contact pressure further reducing variations in blotting trials. After the TLC plates were sprayed with solvent, the TLC plate and nanocomposite were mated, and after the specified blotting time, the TLC plate and nanocomposite were manually separated.

Imaging with STT. Prior research has shown the effectiveness of sample translation in significantly reducing photodegradation of analyte and SERS substrate.[42] Unlike engineered substrates that exhibit good morphological reproducibility,[34−39] random morphology substrates exhibit inhomogeneity and even hot spots that can rise to single molecule sensitivity but can represent an unwanted complication as well. In the case of Ag–polymer nanocomposites, rastering point by point over the substrate can result in an order of magnitude variation of SERS signal for uniformly analyte-coated substrate, with that variability effectively averaged out with circular-STT.[42] In this work, we aim to image TLC plates that inherently have heterogeneity (the separated sample spots) that must be preserved without introducing substrate related artifacts. So, a linear translational device that is compatible with this situation was employed. The linear-STT was effective at reducing photodegradation and improving reproducibility of the SERS signals brought about by substrate inhomogeneity. For example, a nanocomposite was exposed to ATP to create a monolayer and then thoroughly rinsed before being interrogated via SERS imaging with a RSD value of 23% across the nanocomposite. This same area was interrogated again using the linear-STT resulting in a RSD of 7.55%, indicating more than a 3-fold reduction in RSD in intensity across the nanocomposite. In TLC-SERS experiments, the blotted nanocomposite is imaged with the back-and-forth motion of the linear-STT occurring perpendicular to the development direction. This artificially distorts the spot slightly in the nondevelopment direction but leaves the chromatographically significant dimension unaffected.

System Optimization. *Blotting Solvent Selection.* Four conventional reverse-phase solvents, water and the organic modifiers ethanol, methanol, and acetonitrile, were investigated to determine their applicability for conformal blotting. These four solvents exhibit very little SERS background and thus are

dx.doi.org/10.1021/ac303710q | Anal. Chem. 2013, 85, 3991−3998

appropriate for this application. The organic modifiers have varying physical properties significant to conformal blotting such as evaporation rate and strength of solvent. The organic modifiers are all known to be compatible with chromatographic reversed phases. The polarity index (p') values for ethanol, methanol, and acetonitrile are 4.3, 5.1, and 5.8,[45] respectively (see Table 1), and the visually estimated contact angles with cured PDMS for water and the organic solvents were roughly 90° and 40°, respectively, indicating a compatibility with the nanocomposite films.

The evaporation rate (see $T_{1/2}$ values in Table 1) roughly determines the length of time that the conformal blotting can occur because the solvent provides a medium for the analyte to transfer from the TLC plate to the nanocomposite. The expected steps are (i) solubilize the analyte (desirable small solvent−TLC phase capacity factor, k'), (ii) diffusional transfer within solvent to the PDMS surface, (iii) partitioning with the PDMS (desirable large solvent−PDMS k'), and (iv) affinity for and adsorption onto the metal surface (very analyte dependent). It is important to note that the metal is slightly submerged in the phase-separated surface layer of the PDMS (see ref 40 for details). In addition, a potentially important factor in this process of transferring analyte to the nanocomposite is swelling of PDMS by common solvents as has been reported by Whitesides and co-workers.[46] As seen in the table, vapor pressure alone does not determine evaporation rate. The dispersion of the solvent within the porous TLC phase is likely an important factor in determining the length of time the solvent is available to assist transfer analyte to the nanocomposite.

For most analytes, the lower the polarity index of the solvent, the higher the degree of solvation. Ethanol was chosen because of its low p' and low evaporation rate. Other solvents, such as methanol or acetonitrile, could have been chosen to match the specific analytes. While the best solvent is analyte dependent, it also involves a compromise, since an ability to very efficiently solubilize from the TLC phase may reduce the partitioning into the PDMS. Selection of a specific solvent to match a correlating analyte is expected to influence the analytical performance metrics (see below); nevertheless, we have focused on ethanol over the other possible solvents in this initial report.

Optimization of Conformal Blotting. The optimum conditions for blotting were determined using ATP as the analyte. Once again, the TLC plates were exposed to analyte to create a uniform monolayer. Pressure applied to the TLC/nanocomposite system for conformal blotting was tested first because excessive pressure damaged the nanocomposite as clearly observed visually, resulting in less Raman enhancement or no enhancement at all. The optimum pressure for conformal blotting was established at 6 psi using a blotting time of 5 min. Not only did this lead to the maximum SERS intensity, but it also exhibited the lowest RSD in acquired signals (see Table 2). By using the optimum pressure, the amount of time the TLC plate and nanocomposite were contacted was investigated. Intensity as a function of time exhibited a nonlinear trend and began to plateau around 15 min (see Table 3). If needed, conformal blotting could be performed for increased durations of time for trace analysis. Finally, the amount of solvent applied to the TLC plate (see the Experimental Section) was examined. Varying the amount of solvent had very little effect on conformal blotting leading to similar recorded intensities as long as the TLC plate was wetted enough. This probably occurs because the solvent provides a medium for the analyte to transfer from the TLC plate onto the nanocomposite, but the amount of solvent does not affect that equilibrium. While evaporation rate was studied from the TLC plate as seen in Figure 2, it is expected that the evaporation rate decreases significantly after the TLC plate and nanocomposite make contact.

Table 2. Pressure Applied

	6 psi	9 psi	12 psi	15 psi
average	0.70	0.50	0.35	0.50
%RSD (n = 3)	4.1	29	66	90

Table 3. Time (min)

	3	5	7	9	11	13	15
average	0.034	0.11	0.28	0.59	0.76	0.79	0.8
% RSD (n = 3)	30	7.9	15	3.1	5.5	3.3	7.7

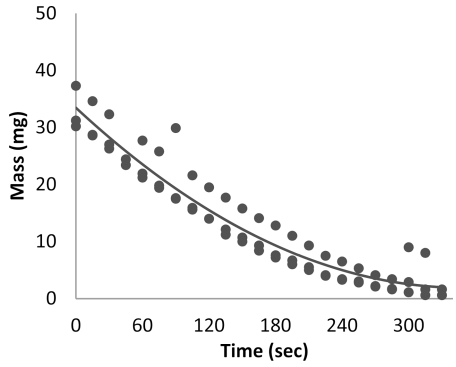

Figure 2. Evaporation rate plot for ethanol. Additional solvent data/properties can be found in Table 1 (n = 3).

Analytical Detection Metrics. By using these optimized blotting conditions and circular-STT, the RSD for an ATP band was better than 10% (ATP, 1128 cm^{-1} band) as seen in Figure 3. Signal acquisition parameters were studied toward the goal of establishing the best calibration and limits of detection for the test analytes. Using Rh6G, laser power and acquisition time were investigated. In SERS imaging, increasing laser power or increasing exposure time of the detector can lead to improved spectra, but overexposure may result in degradation of both the substrate and analyte. The former can be visually observed with nanocomposite substrates, and the latter often is evidenced by broad carbonaceous bands and poor reproducibility.[42] Analysis of Rh6G at a concentration of 3×10^{-6} M using different laser powers is shown in Table 4 at signal acquisition times of 1 s. The circular-STT technique is used here to determine the average peak signal. The Rh6G 595 cm^{-1} peak area is the band analyzed for all of Table 4. At higher laser powers, there was noticeable degradation of the overall spectra resulting in broader peaks, smaller intensities, and disappearance of certain spectral features. At lower laser powers, the spectra were characteristic of customary Rh6G spectra but were low in intensity. The band area trend in terms of signal acquisition time is predictable (see Table 4). The more laser exposure to the sample, the more sample degradation. The table contains peak areas that were normalized and directly correlate to the peak intensity. By combining these optimized parameters, laser

dx.doi.org/10.1021/ac303710q | Anal. Chem. 2013, 85, 3991−3998

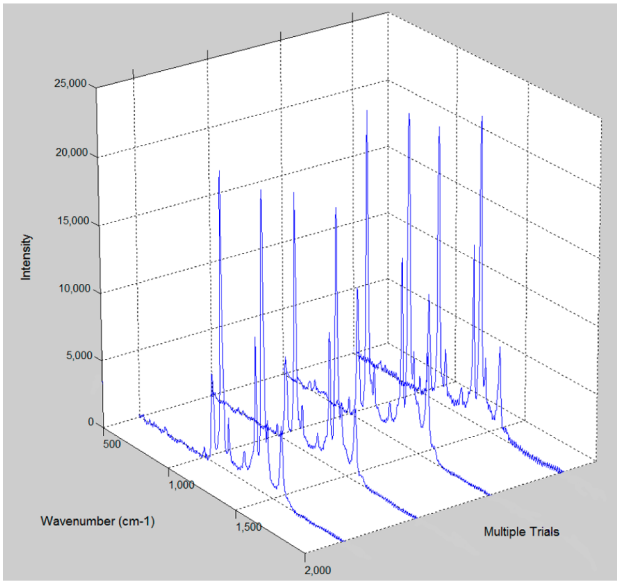

Figure 3. Reproducibility study yielding a %RSD of 9.1 (ATP band area 1128 cm^{-1}). Studies of conditions for conformal blotting of ATP can be found in Tables 2 and 3.

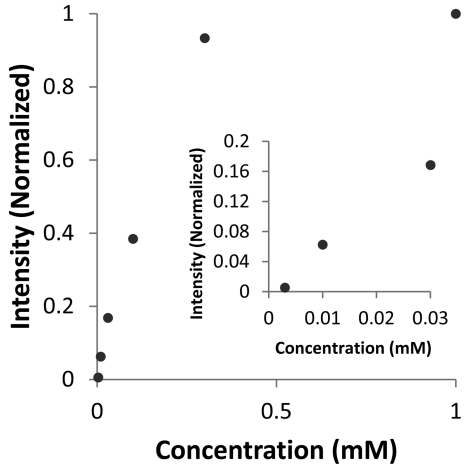

Figure 4. Calibration plot for blotting of Rh6G (insert is a blow up of low concentrations). Peak intensity of 595 cm^{-1} band in acquired spectra is plotted. Additional signal acquisition data is presented in Table 4.

power and acquisition time, optimal limits of detection were established.

The limits of detection were established at 1.47×10^{-7} M for MGITC, 2.20×10^{-7} M for ATP, and 2.74×10^{-6} M for Rh6G. These values were determined using a laser power of 2.5 mW and an acquisition time of 10 s. A short calibration plot was created using lower concentrations samples of the specific analyte. By using a linear trend fit, the data was extrapolated to a concentration with a signal-to-noise ratio of 2 marking the limit of detection for each analyte. Acquisition time could be increased substantially; however, when raster imaging over large areas, the analysis time could be prohibitively long. The limit of detection may be improved for these compounds and others by selecting a specific solvent for conformal blotting that best matches the physical properties of the compound. Prior studies by our group have shown that sorption of aromatic compounds, analogues for environmental pollutants, can be influenced by pH and available counterions (e.g., nitrate, sulfate, carbonate, and phosphate).[47] The counteranion of the MGITC is perchlorate (ClO_4^-) that is a strong oxidizer that may lead to oxidation of the silver and a higher limit of detection. In Figure 4, a full calibration plot for the Rh6G is demonstrated using an acquisition time of 1 s and laser power of 10 mW. Characteristic of SERS, a plateau is approached at high concentrations as a result of saturation of the SERS active metal surface.[48]

Conformal blotting was compared to directly dipping the nanocomposites in the analyte to investigate the efficiency of conformal blotting. In Table 4, the blotting-to-dipping signal ratio can be seen. At low concentrations, conformal blotting is very efficient and produced a signal equivalent to that obtained when the nanocomposite was dipped directly in the same concentration. Conversely, the blotting process appears to be very inefficient at high concentrations. We believe this is misleading because the TLC plate becomes saturated more easily than the nanocomposite film, which is largely composed of PDMS, a high capacity solid-phase extractor.[41,42] Thus, at high concentrations, the available Rh6G on the TLC plate for blotting is considerably less than expected whereas direct dipping of the nanocomposite material into the same Rh6G solution is very efficient.

Analyte TLC Spot Experiments. *Blotting-Related Dispersion.* An important aspect of all chromatographic processes is band (or spot) dispersion that leads to larger plate height (H), diminished resolution, and dilution-related loss in detection sensitivity. While factors that contribute to H are extremely complex in TLC, the treatment by Guiochon and Antoine[49] is generally regarded as comprehensive and is based on the validity of the Knox equation that is common to HPLC theory. Thus, eddy diffusion, axial diffusion, and resistance to mass transfer are expected to be relevant. Similarly, non-separation effects must be considered as sources of dispersion. Typically, the sample spotting process can be thought to be one such factor. However, relative to the work reported herein, we must consider the blotting process and its effect on the size of the TLC spot when transferred to the nanocomposite. Blotting-related spot dispersion was examined by comparing undeveloped Rhodamine 6G spots: fluorescence on the TLC plate and SERS on the nanocomposite film. Linear-STT was employed to

Table 4. Factors Influencing Rhodamine 6G Intensity

						limit of detection	
time (s)	peak area (norm)	laser power (mW)	peak area (norm)	conc (mM)	blot/dip ratio	sample	LOD (μM)
1	0.12	0.0011	0.005	1	0.03	Rh6G	2.74
2	0.23	0.0094	0.059	0.3	0.03	MGITC	0.147
5	0.53	1.14	0.49	0.1	0.17	ATP	0.220
10	1.0	2.89	1.0	0.03	1.3		
		5.66	0.86	0.01	3.5		

dx.doi.org/10.1021/ac303710q | *Anal. Chem.* 2013, 85, 3991−3998

ensure uniformity throughout the nanocomposite while not distorting the spot in the direction that would be used in development. Rhodamine 6G at a concentration of 10^{-4} M was spotted onto a TLC plate and allowed to dry at room temperature. By using an argon laser (488 nm), fluorescence of the undeveloped spot was measured as seen in Figure 5. The

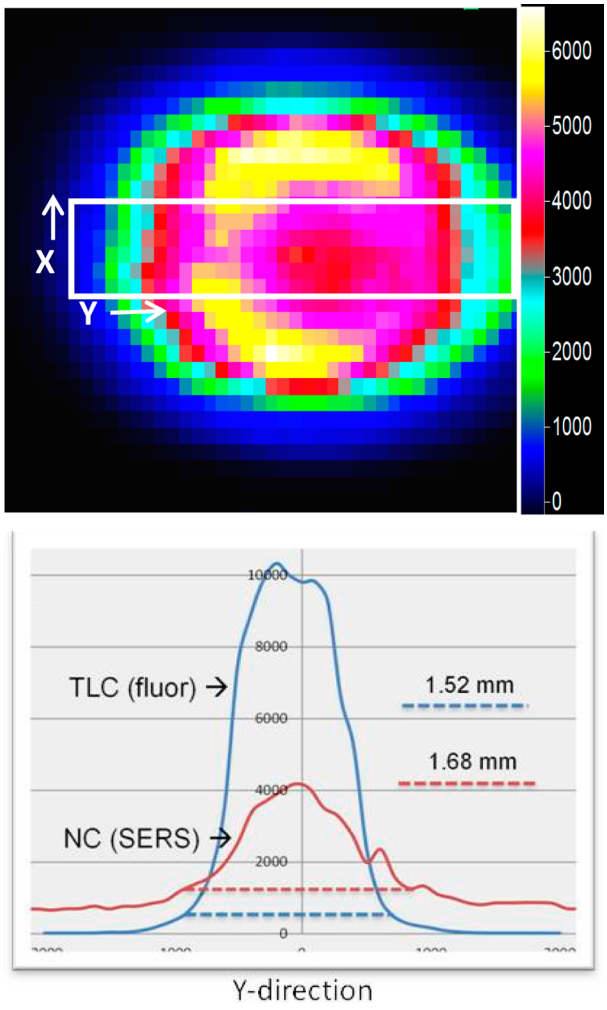

Figure 5. (top) Complete raster plot for typical undeveloped spot of Rh6G on a TLC plate (fluorescence). The incremental jumps were 100 μm in each direction. Linear-STT was applied in the x direction hence creating the elliptical appearance of the spot. The traces below compare the fluorescence width of a spot (undistorted y direction) of a spot on a TLC and the SERS response after blotting that spot onto a nanocomposite (NC) substrate (the rectangle in the raster plot highlights the region of the raster used).

slightly elliptical appearance of the spot is due to the linear-STT movement of 500 μm. The spot was then conformally blotted onto the nanocomposite using the optimized procedure, and the SERS image was obtained. The dried spot on the TLC plate is expected to be stable. However, while in ethanol during the blotting, one can expect some diffusional and perhaps slight convection-related broadening upon plate−nanocomposite contact. As seen in Figure 5, the increase of the width of the spot was approximately 10% indicating that diffusion through conformal blotting is present but not in significant amounts. Rh6G is known to adsorb strongly to the metal. Analytes without such strong adhesion may diffuse while in the PDMS phase, but if the detection is performed within a relatively short period of time, this should be minimal. A similar situation was demonstrated in prior work when the nanocomposite material was molded into a μ-fluidic platform and used for electrophoretic separations.[48]

Separation with Three-Dimensional Detection. A separation of the three test analytes, MGITC, Rh6G, and ATP at concentrations of 10^{-6} M, 10^{-4} M, and 10^{-3} M, respectively, was carried out on a TLC plate using pure ethanol as the mobile phase. The mixture of analytes was spotted onto the TLC plate using an HPLC syringe. After the solvent traveled roughly 2 cm beyond the original sample spot, the TLC plate was removed and allowed to dry at room temperature before being conformally blotted using the optimized conditions. Fluorescence and visual identification of analytes on the TLC plate indicate R_f values of 0.75, 0.43, and 0.28 for ATP, Rh6G, and MGTIC, respectively. This was confirmed using SERS imaging, as seen in Figure 6, by focusing on a specific excitation band for each analyte, 778 cm^{-1} for MGITC, 1128 cm^{-1} for ATP, and 595 cm^{-1} for Rh6G. In both the three-dimensional (3D) plot and spectrally specific chromatogram, it is apparent that the ATP thoroughly separated from the Rh6G and MGITC. However, the Rh6G and MGITC did not exhibit thorough separation resulting in overlapping chromatographic bands due to poor resolution. R_f values are not always a viable option of qualitative analysis; thus, SERS can be employed to identify components. Moreover, quantitative analysis is possible even for overlapping components based on their specific, individual spectral features offsetting a lack of spatial resolution. The efficiency for this conventional TLC separation (developed ATP spot) is only roughly 400 plates underscoring the importance of using an information rich technique to analyze unresolved spots on the developed plate. Previous research by our group has shown that is it possible to distinguish analytes from each other in an aqueous mixture.[50] Our system has many different applications to TLC because the separations can take place on any 2D planar separation medium. Though we used reverse-phase TLC, one could employ many different forms of TLC such as normal phase, special phases (i.e., modification of SiO_2 gel, ion-pairing, molecular imprinted polymers, electrospun polymers), or highly ordered lithographically prepared pillar arrays.[51−53]

■ CONCLUSION

In this report, we have demonstrated the possibility of coupling TLC with SERS through conformal blotting. The unique attributes of Ag−PDMS nanocomposites as pliable and highly SERS-active substrates are exploited. Optimization of blotting led to the efficient transfer of the analyte from the TLC plate onto the nanocomposite substrate with little spot dispersion and good sensitivity and reproducibility. Limited spatial separation can be overcome by SERS imaging, an information rich technique, which enhances both quantitative and qualitative information, potentially expanding applications to samples that are more complex than normally possible in TLC. Note that, while the test analytes used herein are Raman active that are often used in the development of many SERS approaches, other Raman active analytes should be applicable. Additionally, conformal blotting effectively isolates separation conditions from that required for detection. Thus, this versatile approach is expected to be applicable to many different types of 2D planar separation platforms and separation media.

dx.doi.org/10.1021/ac303710q | *Anal. Chem.* 2013, 85, 3991−3998

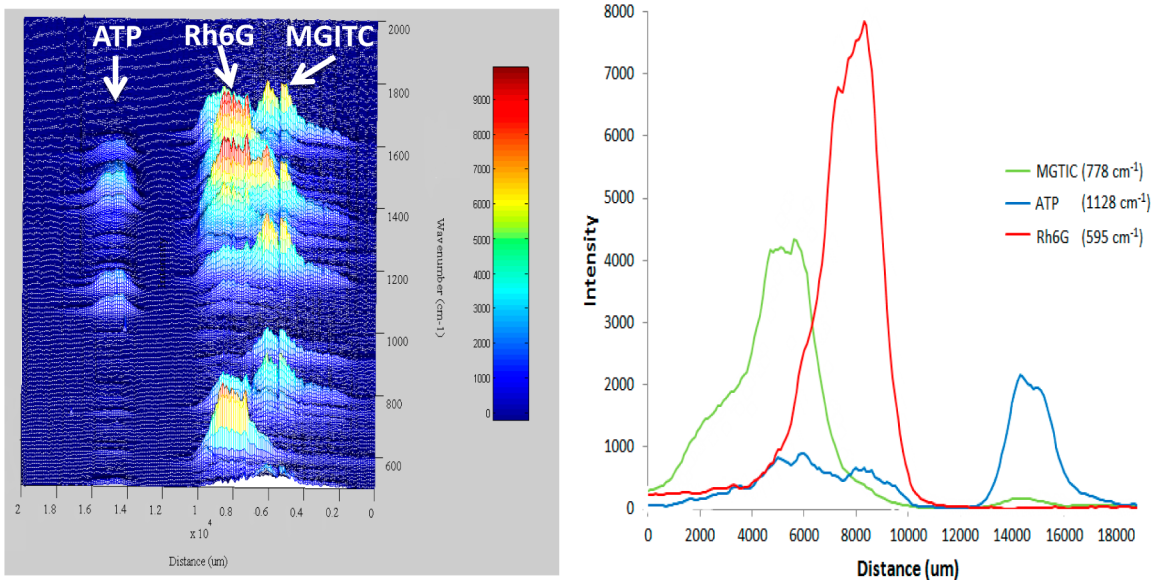

Figure 6. 3D chromatogram showing the separation of MGITC, Rh6G, and ATP with associated spectra. A chromatogram of the three test compounds based on a spectral peak specific to each compound is also shown.

AUTHOR INFORMATION

Corresponding Author

*Phone: (865) 974-8023; e-mail: msepaniak@utk.edu.

Notes

The authors declare no competing financial interest.

ACKNOWLEDGMENTS

This material is based on work supported in part by the National Science Foundation under Grant CHE-1144947 with the University of Tennessee. A portion of this research was conducted at the Center for Nanophase Materials Sciences, which is sponsored at Oak Ridge National Laboratory by the Scientific User Facilities Division, Office of Basic Energy Sciences, U.S. Department of Energy. Additional support was provided by the University of Tennessee, Knoxville, Chancellor's Honors Program.

REFERENCES

(1) Poole, S. K.; Poole, C. F. *J. Chromatogr., A* **2010**, *19*, 2648−2660.
(2) Poole, C. F. *J. Chromatogr., A* **2003**, *1000*, 963−984.
(3) Sherma, J. *Anal. Chem.* **2004**, *76*, 3251−3262.
(4) Sherma, J.; Fried, B. *Handbook of Thin-Layer Chromatography*, 3rd ed.; Marcel Dekker: New York, 2003.
(5) Poole, C. F.; Poole, S. K. *Chromatography Today*; Elsevier: Amsterdam, The Netherlands, 1991; pp 649−728.
(6) Cserhati, T. *Biomed. Chromatogr.* **2002**, *16*, 303−310.
(7) Orinak, A.; Arlinghaus, H. F.; Vering, G.; Justinova, M.; Orinakova, R.; Turcaniova, L.; Halama, M. *J. Planar Chromatogr.−Mod. TLC* **2003**, *16*, 23−27.
(8) Istvan, K.; Keresztury, G.; Szep, A. *Spectrochim. Acta, Part A* **2003**, *59*, 1709−1723.
(9) Jing, C.; Abell, J.; Huang, Y.; Zhao, Y. *Lab Chip* **2012**, *12*, 3096−3102.
(10) Wang, Y.; Zhang, J. Z.; Ma, X. Y. *Spectrosc. Spectral Anal.* **2004**, *24*, 1373.
(11) Brosseau, C. L.; Gambardella, A.; Casadio, F.; Grzywacz, C. M.; Wouters, J.; Duyne, R. P. *Anal. Chem.* **2009**, *81*, 3056−3062.
(12) Walworth, M.; Stankovich, J.; Van Berkel, G.; Schultz, M.; Minarik, S. *Rapid Commun. Mass Spectrom.* **2012**, *26*, 37−42.
(13) Minami, Y.; Yokoi, S.; Setoyama, M.; Bando, N.; Takeda, S.; Kawai, Y.; Terao, J. *Lipids* **2007**, *42*, 1055−1063.
(14) Kawai, Y.; Miyoshi, M.; Moon, J.; Terao, J. *Anal. Biochem.* **2006**, *360*, 130−137.
(15) Dieringer, J. A.; McFarland, A. D.; Shah, N. C.; Stuart, D. A.; Whitney, A. V.; Yonzon, C. R.; Young, M. A.; Zhang, X.; Van Duyne, R. P. *Faraday Discuss.* **2006**, *132*, 9−26.
(16) Kneipp, K.; Kneipp, H. *Appl. Spectrosc.* **2006**, *60*, 322A.
(17) Moskovits, M. *J. Chem. Phys.* **1978**, *69*, 4159.
(18) Moskovits, M. *Rev. Mod. Phys.* **1985**, *57*, 783.
(19) Kneipp, K.; Kneipp, H. *Isr. J. Chem.* **2006**, *46*, 299−305.
(20) Kneipp, K.; Wang, Y.; Kneipp, H.; Perelman, L. T.; Itzkan, I.; Dasari, R. R.; Feld, M. S. *Phys. Rev. Lett.* **1997**, *78*, 1667.
(21) Kneipp, K.; Kneipp, H.; Deinum, G.; Itzkan, I.; Dasari, R. R.; Feld, M. S. *Appl. Spectrosc.* **1998**, *52*, 175.
(22) Kneipp, K.; Kneipp, H.; Kartha, V. B.; Manoharan, R.; Deinum, G.; Itzkan, I.; Dasari, R. R.; Feld, M. S. *Phys. Rev. E.* **1998**, *57*, R6281.
(23) Zou, S. L.; Schatz, G. C. *Chem. Phys. Lett.* **2005**, *403*, 62.
(24) Gopinath, A.; Boriskina, S. V.; Reinhard, B. M.; Dal Negro, L. *Opt. Express* **2009**, *17*, 3741−3753.
(25) Musick, M. D.; Keating, C. D.; Lyon, L. A.; Botsko, S. L.; Pena, D. J.; Hollay, W. D.; McEvoy, T. M.; Richardson, J. N.; Natan, M. J. *Chem. Mater.* **2000**, *12*, 2869−2881.
(26) Park, S.-H.; Im, J.-H.; Im, J.-W.; Chun, B.-H.; Kim, J.-H. *Microchem. J.* **1999**, *63*, 71−91.
(27) Lacy, W. B.; Olson, L. G.; Harris, J. M. *Anal. Chem.* **1999**, *71*, 2564−2570.
(28) Mulvaney, S. P.; He, L.; Natan, M. J.; Keating, C. D. *J. Raman Spectrosc.* **2003**, *34*, 163−171.
(29) Reilly, T. H., III; Corbman, J. D.; Rowlen, K. L. *Anal. Chem.* **2007**, *79*, 5078−5081.
(30) Li, J.; Fang, Y. *Spectrochim. Acta, Part A* **2007**, *66A*, 994−1000.
(31) Murgida, D.; Hildebrandt, P. *Top. Appl. Phys.* **2006**, *103*, 313−334.
(32) Pristinski, D.; Tan, S.; Erol, M.; Du, H.; Sukhishvili, S. *J. Raman Spectrosc.* **2006**, *37*, 762−770.
(33) Qian, X. M.; Ansari, D.; Nie, S. *Proc. SPIE* **2007**, *6448*, 1−12.
(34) Oran, J. M.; Hinde, R. J.; Abu Hatab, N.; Sepaniak, M. J. *J. Raman Spectrosc.* **2008**, *39*, 1811−1820.
(35) Wells, S. M.; Polemi, A.; Lavrik, N. V.; Shuford, K. L.; Sepaniak, M. J. *Chem. Commun.* **2011**, *47*, 3814−3816.
(36) Bhandari, D.; Kravchenko, I. I.; Lavrik, N. V.; Sepaniak, M. J. *J. Am. Chem. Soc.* **2011**, *133*, 7722−7724.
(37) Green, M.; Liu, F. M *J. Phys. Chem. B* **2003**, *107*, 13015−13021.

(38) Yan, B.; Thubagere, A.; Premasiri, W. R.; Ziegler, L. D.; Dal Negro, L.; Reinhard, B. M. *ACS Nano* **2009**, *3*, 1190−1202.
(39) Haynes, L. C.; Van Duyne, R. P. *J. Phys. Chem. B* **2003**, *107*, 7426−7433.
(40) De Jesus, M. A.; Giesfeldt, K. S.; Sepaniak, M. J. *J. Raman Spectrosc.* **2004**, *35* (10), 895−90.
(41) Giesfeldt, K. S.; Connatser, R. M.; De Jesús, M. A.; Lavrik, N. V.; Dutta, P.; Sepaniak, M. J. *Appl. Spectrosc.* **2003**, *57*, 1346.
(42) De Jesus, M. A.; Giesfeldt, K. S.; Sepaniak, M. J. *Appl. Spectrosc.* **2003**, *57*, 428−438.
(43) Henzel, U. B. *Journal of Chromatography Library*; Zlatkis, A., Kaiser, R. E., Eds.; Elsevier: Amsterdam, The Netherlands, 1977; Vol. *9*, Chapter 8.
(44) White, R. L. *Anal. Chem.* **1985**, *57*, 1819.
(45) Snyder, L. R. *Techniques of Chemistry*, 2nd ed.; Weissberger, A., Perry, E. S., Eds.; Wiley-Interscience: New York, 1978; Vol. *III*, Part I, Chapter 2.
(46) Lee, J. N.; Park, C.; Whitesides, G. M. *Anal. Chem.* **2003**, *75*, 6544−6554.
(47) DeJesus, M. A.; Giesfeldt, K. S.; Sepaniak, M. J. *Appl. Spectrosc.* **2004**, *58*, 1157−1164.
(48) Connatser, R. M.; Cochran, M.; Harrison, R. J.; Sepaniak, M. J. *Electrophoresis* **2008**, *29*, 1441−1450.
(49) Guiochon, G.; Antoine, S. *J. Chromatogr. Sci.* **1978**, *16*, 470−481.
(50) Bhandari, D.; Walworth, M. J.; Sepaniak, M. J. *Appl. Spectrosc.* **2009**, *63*, 571−578.
(51) Lavrik, N. K.; Taylor, L.; Sepaniak, M. J. *Lab-on-a-Chip* **2010**, *10*, 1086−1094.
(52) DeMalsche, W.; Eghbali, H.; Clicq, D.; Vangelooven, J.; Gardeniers, H.; Desmet, G. *Anal. Chem.* **2007**, *79*, 5915.
(53) Clark, J. E.; Olesik, S. V. *Anal. Chem.* **2009**, *81*, 4121−4129.